

Final Transfer Function of the Lares Retroreflector Array

I.D No. 3047

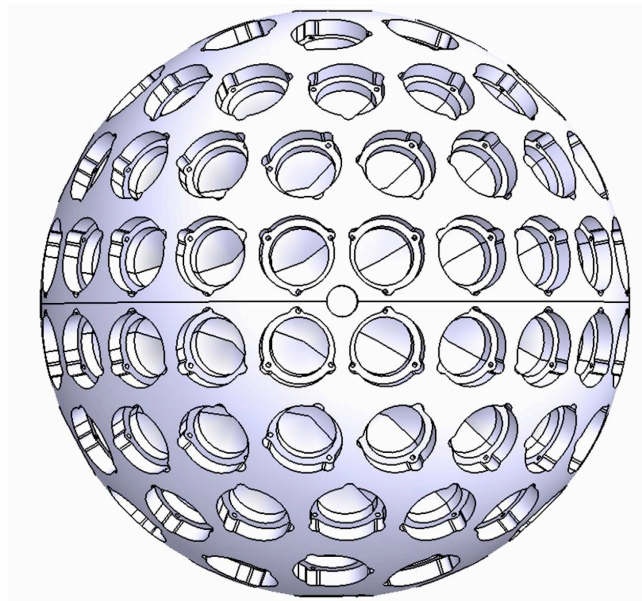
David A. Arnold

94 Pierce Rd

Watertown, MA 02472

david-arnold@earthlink.net

Smithsonian Astrophysical Observatory (Retired)



Abstract. The final transfer function of the LARES retroreflector array has been computed including the geometry of the array, reflectivity of an individual cube corner, variation of the transfer function with various parameters, cross section, range correction, average return pulse shape, effect of optical coherence, and estimated accuracy of the results. The average cross section is about 3.3 million sq m and the average range correction is about 127.5 mm.

This poster contains excerpts from the paper which will be available after review on the ILRS website at http://ilrs.gsfc.nasa.gov/about/reports/other_publications.html.

Table of Contents of the full paper

- 1 Introduction
- 2 Cube corner specifications
- 3 Geometry of the array
- 4 Method of computing the transfer function
- 5 Signal strength computation
- 6 Cube corner reflectivity
- 7 Variation of the transfer function
- 8 Reflectivity histogram
- 9 Array reflectivity
- 10 Range correction
- 11 Effect of optical coherence
- 12 Accuracy of the results
- 13 Acknowledgments
- 14 References

Distribution of Dihedral Angle Offsets

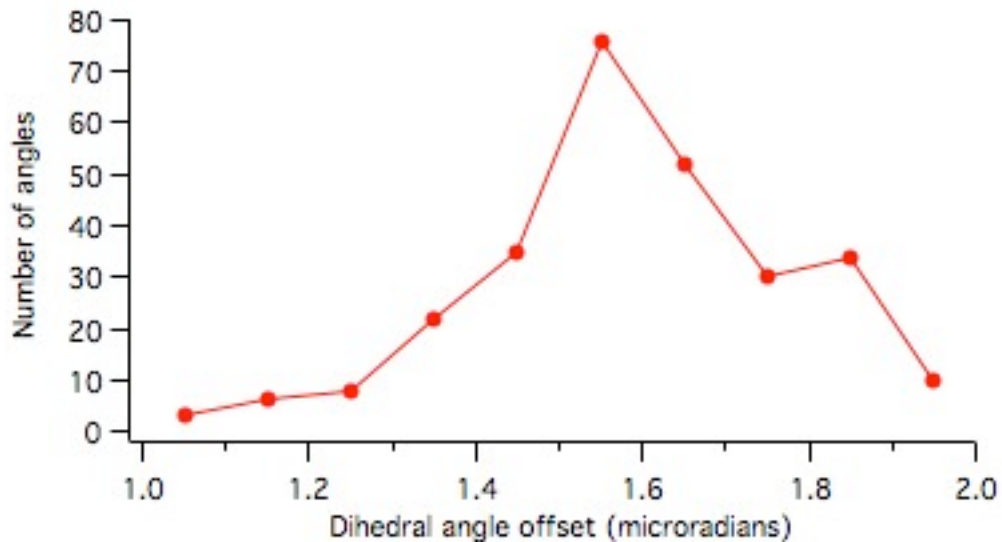


Figure 2.1. Distribution of the dihedral angle offsets (.1 arcsec bins). The average offset is 1.58 arcsec that is close to the nominal 1.50 arcsec offset. There are 92 cubes with three angles each for a total of 276 angles.

Total Internal Reflection

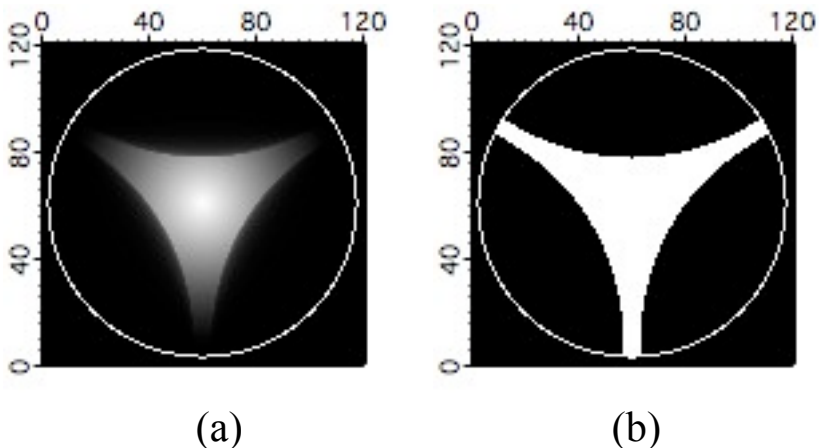


Figure 6.1. Loss of total internal reflection in an uncoated cube. Part (a) is the total reflected energy vs incidence angle. Part (b) is the region where total internal reflection occurs. The circle is the absolute cutoff angle of the cube corner (57 deg). There are real back edges pointing up at $\theta = 90$ and at $\theta = -30$ and $\theta = -150$ deg. Each point in the matrix represents an incidence angle (θ, ϕ) where

$$\theta = \tan^{-1}(y/x) \tag{6.1}$$

and

$$\phi = \sqrt{x^2 + y^2} \tag{6.2}$$

Pulse Histogram

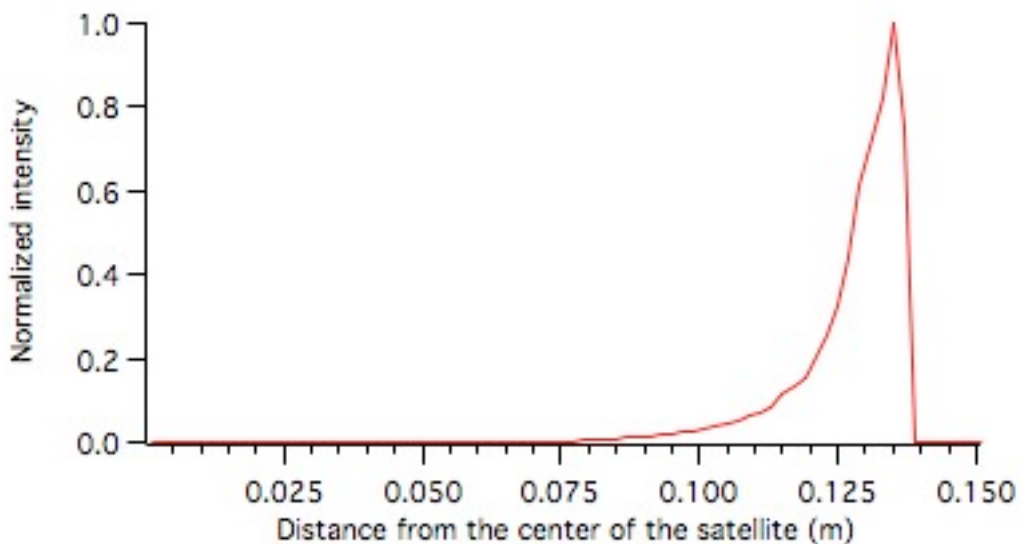


Figure 8.1. Histogram of the return pulse from Lares (2 mm bins).

Average cross section for circular and linear polarization

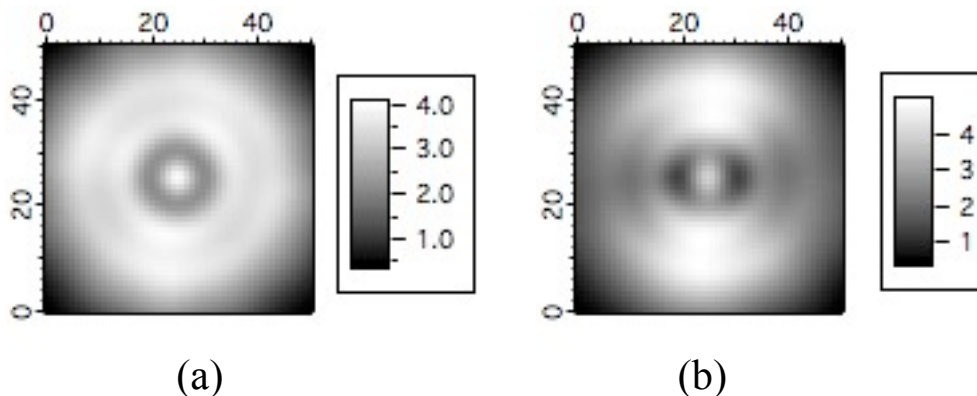


Figure 9.1. Average cross section matrix (million sq m) over 1080 incidence angles for circular polarization (a) and linear vertical polarization (b). The dihedral angle offset is 1.5 arcsec. The cross section matrix has circular symmetry for circular polarization. However, it is asymmetric for linear vertical polarization. The matrix is 51 x 51 elements going from -50 to +50 microradians. ***The average cross section between 30 and 45 microradians is 3.3 million sq meters.***

Average centroid for circular and linear polarization

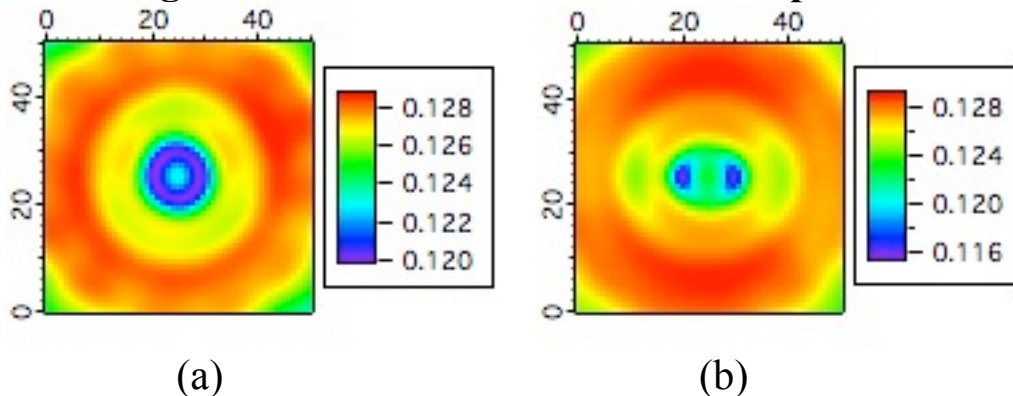


Figure 10.3. Average centroid range correction (m) over 1080 incidence angles for circular polarization (a) and linear vertical polarization (b). The dihedral angle offset is 1.5 arcsec. For circular polarization the pattern has nearly circular symmetry. For linear vertical polarization the pattern is asymmetric. The matrix is 51 x 51 elements going from -50 to +50 microradians.

Range correction vs velocity aberration

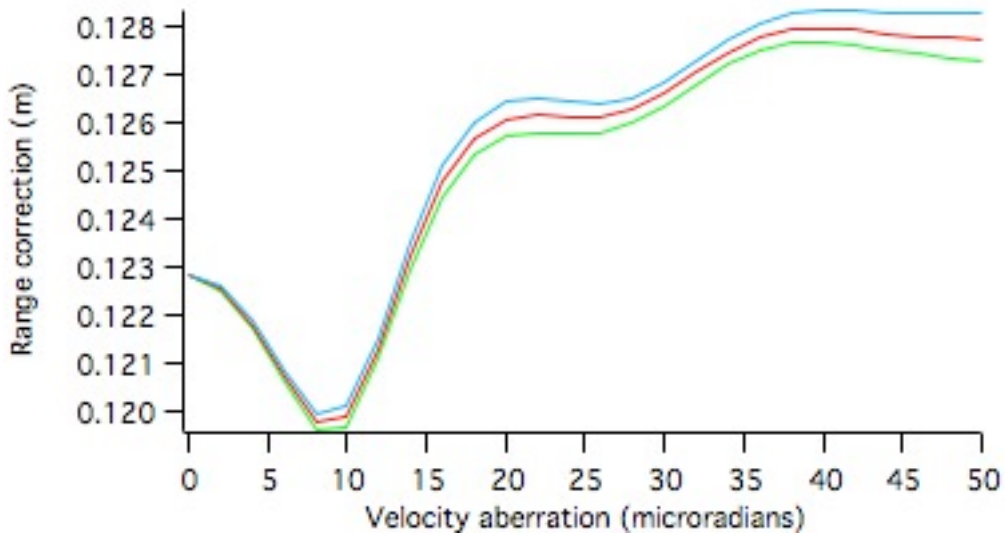


Figure 10.9. Range correction vs velocity aberration averaged over 1080 orientations using the actual dihedral angle offsets for Lares with circular polarization.

Green = minimum around the circle

Red = average around the circle

Blue = maximum around the circle

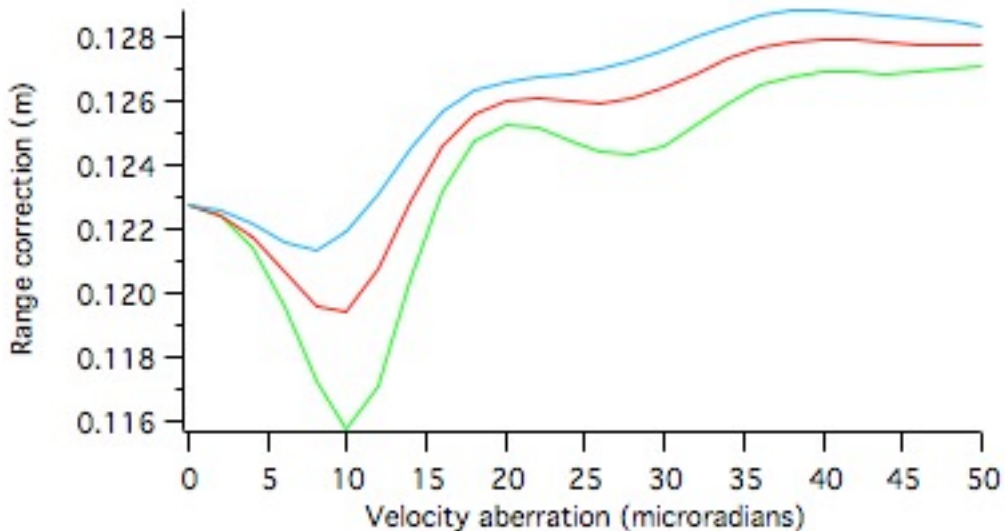


Figure 10.12. Centroid vs velocity aberration averaged over 1080 orientations with actual dihedral angles and linear vertical polarization.

Microrad	Circular(m)	Linear(m)
30.0	0.1265930	0.1263715
32.0	0.1270283	0.1268242
34.0	0.1274531	0.1272825
36.0	0.1277645	0.1276309
38.0	0.1279288	0.1278265
40.0	0.1279638	0.1278839
42.0	0.1279181	0.1278532
44.0	0.1278470	0.1277948
46.0	0.1277905	0.1277519

Table 10.5. Averaged centroid vs velocity aberration for circular and linear polarization with the actual dihedral angle offsets in the 30 - 45 microradian range. ***The average range correction for linear polarization in Table 10.5 over the range from 30 to 45 microradians is 127.4 mm.*** This should be the best estimate.

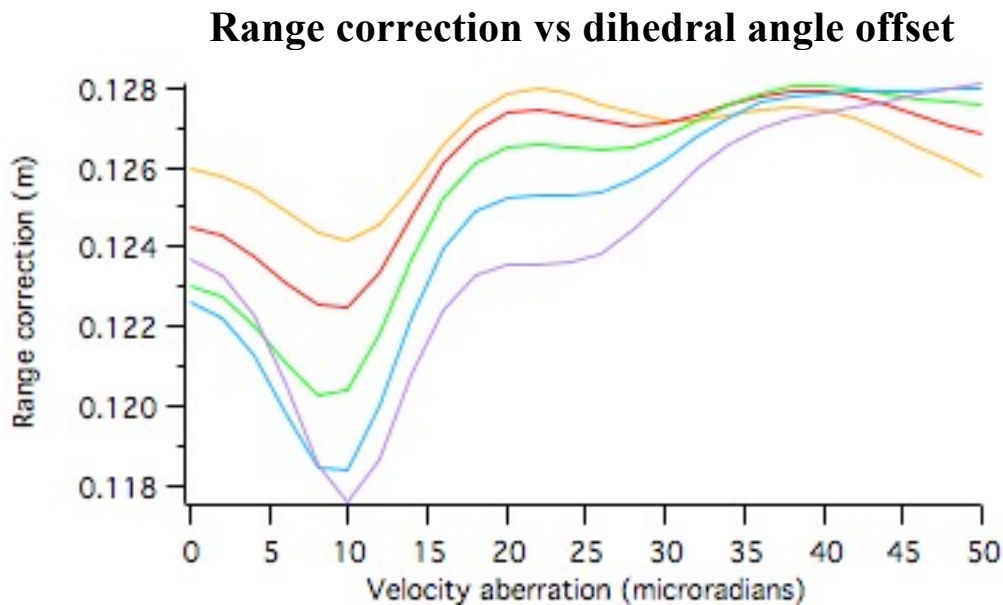


Figure 10.7. Range correction (m) vs velocity aberration (microradians) for 5 different dihedral angle offsets (arcsec).

Color	Arcsec	Centroid (m) in the 30 – 45 microrad annulus
Yellow	1.00	.1273
Red	1.25	.1277
Green	1.50	.1278
Blue	1.75	.1276
Purple	2.00	.1270

Half maximum range correction

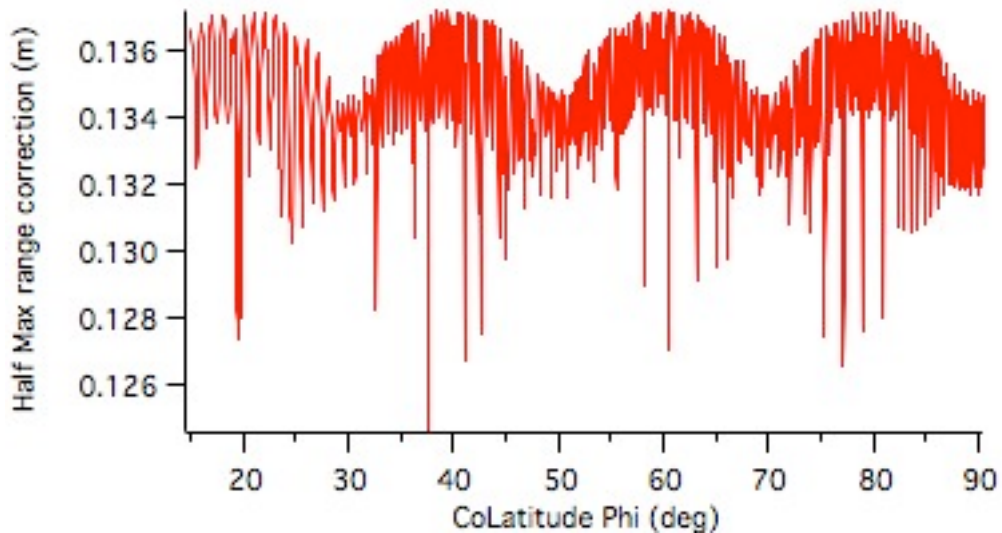


Figure 10.16. Half maximum range correction vs colatitude at velocity aberration (36,0) microradians. The half maximum range depends on the transmitted pulse width that is 30 picoseconds. The minimum is .1246 m, the maximum is .1372 m, $\text{max} - \text{min} = .0126$ m, the average is .1346 m, and the r.m.s. variation is .0018 m (1.8 mm). There is clearly a systematic variation with colatitude. The peaks correspond to incidence angles where the incidence beam is normal to one of the rows of cube corners. The occasional low values are due to irregular pulse shapes where the first peak is less than half the highest peak

The half maximum correction should be representative of leading edge detection systems.

Effect of optical coherence

Probability histograms of the cross section (a), centroid (b), and half max range correction (c) vs distance from the center of the satellite (m) for various transmitted pulse lengths.

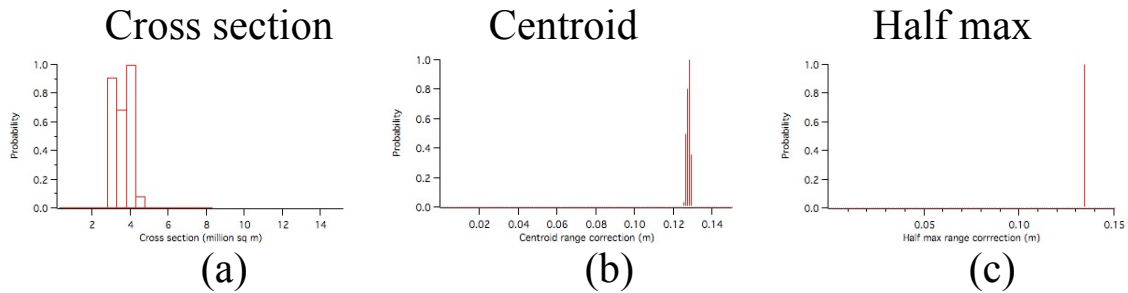


Figure 11.2 Pulse length 10 ps

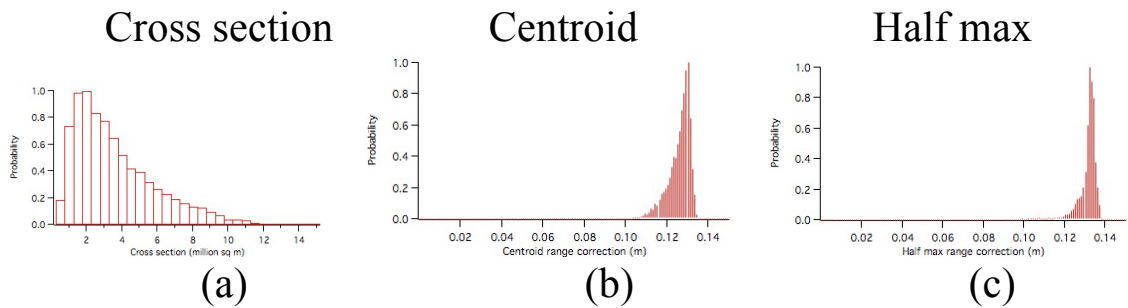


Figure 11.3 Pulse length 100 ps.

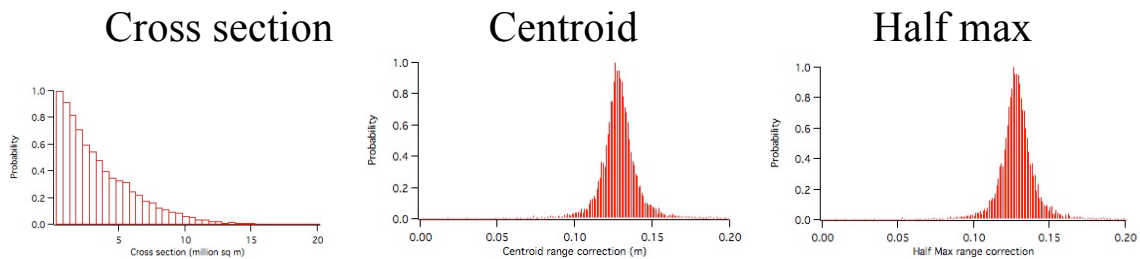
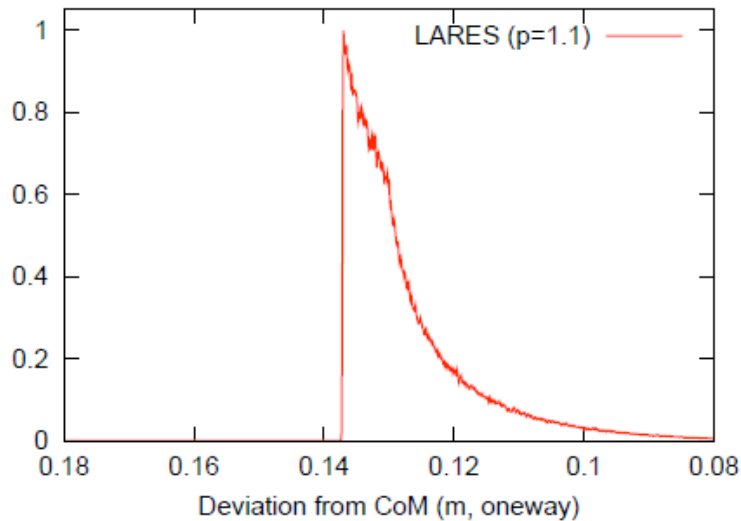


Figure 11.4 Pulse length 10,000 ps.

The probability distribution of the cross section is exponential for long pulse lengths in agreement with theoretical predictions.

Agreement with measured data



Paper ID # 13-0419-otsubo-mmslr.pdf from LW18 on analysis of actual tracking data includes the figure above on slide 11. It shows good agreement with the pulse histogram Fig 8.1 on slide 3 of this poster including the change in slope where loss of total internal reflection begins. The effect of loss of total internal reflection is shown in Fig 6.1 on slide 3 of this poster. The leading edge in the LW18 figure is at .1371 (m) and the centroid is .1275 (m). The maximum computed half max correction in Fig 10.16 on slide 7 of this poster is .1372 (m) and the centroid in Table 10.5 on slide 6 is .1274 (m). The close agreement between the measured and computed values suggests that both may be accurate to .1 mm.

The significance of this agreement is that it might be possible to reduce target induced range biases to the sub-millimeter level by applying a theoretically calculated correction as a function of velocity aberration. In table 10.5 of slide 6 the centroid for linear polarization varies from .12637 (m) to .12788 (m) as a function of velocity aberration, a difference of 1.5 mm. It might be possible to confirm the dependence on velocity aberration by analyzing the experimental data as a function of velocity aberration.